Available online at www.sciencedirect.com
SCIENCE DIRECT®
Polymer 44 (2003) 7007–7019
polymer
www.elsevier.com/locate/polymer

Structural change in the Brill transition of Nylon m/n (1) Nylon 10/10 and its model compounds

Yayoi Yoshioka[a,b], Kohji Tashiro[a,*]

[a]*Department of Macromolecular Science, Graduate School of Science, Osaka University, 1-1 Machikaneyama-cho, Toyonaka, Osaka 560-0043, Japan*
[b]*Technology Research Institute of Osaka Prefecture, Izumi, Osaka 594-1157, Japan*

Received 22 January 2003; received in revised form 3 April 2003; accepted 13 April 2003

Abstract

Structural changes in the Brill transitions of Nylon 10/10 and its model compounds have been investigated by carrying out the temperature-dependent measurements of X-ray diffraction and infrared spectra along with the DSC measurement. The crystal structure at room temperature was found to be the so-called α form with the all-*trans* zigzag methylene segments. When the samples were heated, the infrared progression bands of the methylene segments, which are sensitive to the length of all-*trans* segmental parts, were found to change their spectral patterns in the transition temperature region: the progression bands decreased in intensity and disappeared above the transition region. At the same time several new bands were observed to appear, which were found to correspond to the progression bands of $(CH_2)_7$–$(CH_2)_5$ *trans*-zigzag segments. These spectral changes indicate that the methylene segments were conformationally disordered by an invasion of some *gauche* bonds and as a result the effective length of *trans*-zigzag segments became shorter. This conformational disordering was found to occur more remarkably in the methylene segment of NH–$(CH_2)_{10}$–NH part than the CO–$(CH_2)_8$–CO part. At the same time the infrared bands of amide groups, in particular the bands sensitive to the twisting angles about the CH_2–amide bonds were found to show the remarkable change, indicating the local conformational change from planar-zigzag to twisted form in the CH_2–amide moiety. The frequency shift of amide A band (NH stretching mode) indicated a weakening of intermolecular hydrogen bonds, which however, did not disappear up to the melting region. From these data combined with the X-ray diffraction data, the structural disordering in the Brill transition phenomena was deduced concretely.

Keywords: Nylon; Brill transition; Infrared spectra

1. Introduction

When Nylon 66, for example, is heated up to 210 °C, the triclinic crystal lattice is said to transform to the pseudo-hexagonal lattice as being detected by the X-ray diffraction measurement [1]. This phenomenon is called a Brill transition and can be observed for many kinds of aliphatic nylons. This transition was told to be a thermodynamically 1st-order phase transition. But it was also proposed that a convergence of X-ray reflections into one peak is only apparent and is rather due to the anisotropy of linear thermal expansivity of the crystal lattice i.e. no phase transition occurs substantially [2]. There have been published many papers in which the changes in the crystal lattice parameters were discussed mainly on the basis of X-ray diffraction data [1–17]. But the concrete structural changes, in particular the changes in conformation and packing mode of molecular chains have not yet been revealed well enough because of ambiguous X-ray diffraction data coming from small crystallites. Rather the infrared spectroscopic data may be useful to get more concrete information about the changes in molecular conformation, chain packing structure, hydrogen bonds and so on. By carrying out the analysis of infrared progression bands, which are sensitive to the length of all-*trans* methylene sequences [18–23], the conformation of methylene sequences may be clarified also. But the characterization of the progression bands has not yet been established completely. Quite recently, we succeeded in analyzing a series of progression bands observed for various kinds of nylons and the model compounds [32]. As for the temperature dependence of progression bands, the

* Corresponding author. Tel./fax: +81-6-6850-5455.
E-mail address: ktashiro@chem.sci.osaka-u.ac.jp (K. Tashiro).

0032-3861/$ - see front matter © 2003 Elsevier Ltd. All rights reserved.
doi:10.1016/j.polymer.2003.04.001

qualitative study has just started in recent years [6,23–26] and no details have been revealed about the conformational change. Similarly the amide bands are sensitive to the conformational change of amide part or the twisting angle around the amide–CH_2 bond [33]. Therefore, by combining all of these infrared spectroscopic information with the X-ray diffraction data, the structural change in the whole crystal lattice will be revealed clearly.

In such a trial, it is useful to employ a series of low-molecular-weight model compounds of nylon and to collect more detailed information on the structural changes in the phase transitions, which should be fed back to the parent polymers. However, the study of these model compounds has been limited in number [12,24–31], and no detailed description has not yet been made as to the concrete structural change in the Brill transition phenomenon. In the present paper, we will treat several model compounds of Nylon 10/10 with the following formulae as well as Nylon 10/10 itself.

N1010CC

$$CH_3(CH_2)_9-NHCO-(CH_2)_8-CONH-(CH_2)_9CH_3 \quad (1)$$

N1010NN

$$CH_3(CH_2)_8-CONH-(CH_2)_{10}-NHCO-(CH_2)_8CH_3 \quad (2)$$

N10 $CH_3(CH_2)_8-CONH-(CH_2)_9CH_3$ (3)

Nylon 10/10 $-[CO-(CH_2)_8-CONH-(CH_2)_{10}-NH]_n-$ (4)

We have chosen these compounds as the representatives for investigation of Brill transition of nylons, because they have long methylene segments suitable for the study of the conformational change. Besides the model compounds (1) and (2) are not so simple as N10 (3) and are not so complicated as those having more number of amide groups (for example, $CH_3(CH_2)_9NHCO(CH_2)_8CONH(CH_2)_{10}$-$NHCO(CH_2)_8CH_3$ and so on). As for the model compounds (1) and (2), they are different in the orientation of amide groups, allowing us to know the effects of amide group orientation on the thermal motion and conformation of methylene segments.

Nylon 10/10 was said to show no Brill transition below the melting point [15,16]. As will be shown in a later section, the two main X-ray (100) and (010,110) reflections of the triclinic lattice start to change their positions already about several tens degrees below the melting point and come closer each other by further heating. They are almost merging into one reflection several degrees just below the melting point but disappear finally due to the melting. That is to say, these two reflections do not merge perfectly into one reflection of the pseudo-hexagonal lattice below the melting point, although a further heating by only a few degrees might bring the crystal to the pseudo-hexagonal lattice perfectly if the crystallites could be kept unmelted. Is it really suitable to define the Brill transition simply as one unique temperature point where the perfect convergence of X-ray reflections into one peak occurs? Rather is it impossible to reconsider the Brill transition as an order-to-disorder structural change occurring in a finite temperature region? The structural disordering is found to occur in a relatively wide temperature region even for the low-molecular-weight model compounds as will be shown later. Therefore, the transition in a wide temperature region is not necessarily due to the broad crystallite size distribution characteristic of the semicrystalline nylon sample but maybe reflect any intrinsic behavior of the crystal. The infrared spectra will give us some useful and concrete information about the structural change in molecular chain and packing mode of these chains as will be described in a later section, and should answer us the above-mentioned questions concerning the essential features of the Brill transition.

2. Experimental section

2.1. Samples

Model compounds N1010CC and N1010NN were synthesized by a condensation reaction of 1,8-octandicarboxylic chloride with 1-aminodecane in toluene solution and *n*-decanoyl chloride with 1,10-diaminodecane in cycrohexanone solution, respectively. The recrystallization of these compounds was made from the hot ethanol solution three times, from which the α form was obtained for both the N1010CC and N1010NN. An elementary analysis was made: for N1010CC, C 74.72% (prediction 74.94%), H 12.77% (12.58%), and N 5.81% (5.83%) and for N1010NN, C 74.76% (74.94%), H 12.62% (12.58%), and N 5.89% (5.83%). Nylon 10/10 was kindly supplied by the Shanghai Cellulose Works, Shanghai, China. The preparation of N10 sample was described in a previous paper [25].

2.2. Measurements

The DSC thermograms were measured in the heating process by using a differential scanning calorimeter SEIKO DSC220CU under nitrogen gas atmosphere at the rate of 4 °C/min.

For infrared spectral measurement, a thin film of Nylon 10/10 was prepared by pressing the molten sample between a pair of KBr plates. The thus obtained film was found to be almost the pure α crystalline phase as judged from the infrared spectral patterns. The KBr disks were prepared for the powder samples of model compounds, N1010CC and N1010NN. Temperature dependence of the infrared spectra was measured using a Biorad FTS-60A/896 Fourier-transform infrared spectrometer at the resolution power of 2 cm^{-1}. The temperature dependence of X-ray diffraction

profile was measured by using a Rigaku RINT-Ultima^{+} X-ray diffractometer with a graphite-monochromatized Cu Kα line at the scan speed of 1 °C/min.

3. Results and discussion

3.1. DSC thermograms

Fig. 1 shows the DSC thermograms measured for N10, N1010CC, N1010NN and Nylon 10/10 in the heating process from room temperature. In case of the model compound N10 with one amide group, a small endothermic peak was detected around 50 °C in addition to a larger endothermic peak around 70 °C due to the melting. For N1010CC, smaller and broader peaks corresponding to the phase transitions were observed in the temperature regions of 60 and 90 °C. Enthalpy changes ΔH of the two main endothermic peaks and the melting peak were 88 J/g (summation of the first two broad peaks) and 168 J/g, respectively. The N1010NN showed a shoulder immediately below the melting peak, about 140 °C. The ΔH was estimated ca. 169 J/g for this peak, where the contribution from the shoulder was included. In quite broad region starting from ca. 70 °C, a very small endothermic peak was detected (ΔH ca. 10 J/g), where some thermal motion was considered to occur as will be discussed later. Similar broad change of thermal output was observed also for Nylon 10/10 in the region of 50–140 °C. The structural change in this region will be discussed in a later section. A broad endothermic peak was also observed in the region of 130–195 °C just below the melting peak at 202 °C: ΔH was estimated ca. 46 and 29 J/g, respectively. As seen in Fig. 1, the melting temperature was found to increase remarkably by increasing the number of amide groups by only one from N10 to N1010NN and N1010CC. From the DSC data it may be speculated that the Brill transition occurs in the temperature region of 70–110 °C for N1010CC, 140–190 °C for Nylon 10/10 and immediately below the melting point for N1010NN.

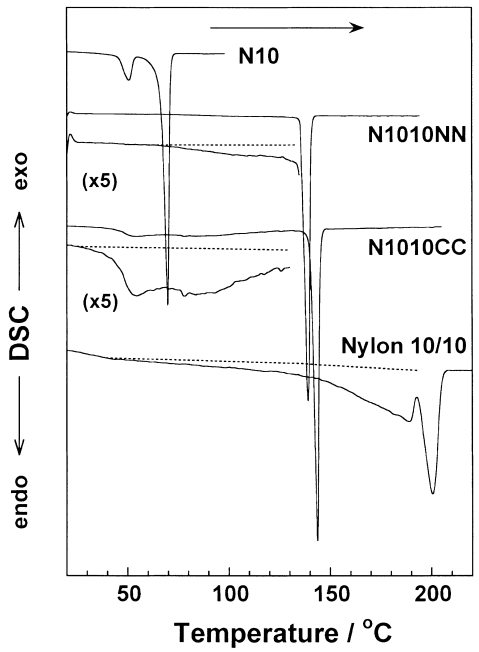

Fig. 1. DSC thermograms of N10, N1010NN, N1010CC and Nylon 10/10 taken in the heating process.

3.2. Temperature dependence of infrared spectra

3.2.1. Amide group bands

Temperature dependence of infrared spectra in the frequency region of 450–800 cm^{-1} is shown in Fig. 2(a)–(c) for N1010CC, N1010NN and Nylon 10/10, respectively. At room temperature Nylon 10/10 and the model compounds showed the infrared bands typical of the planar-zigzag structure of α form: around 580 cm^{-1} [amide VI (C=O out-of-plane mode)] and 680 cm^{-1} [amide V (NH out-of-plane mode)] [34–42]. The infrared bands characteristic of the α form can be observed also around 3310 cm^{-1} [amide A (NH stretching mode)], 1635 cm^{-1} [amide I (C=O stretching mode)], 1535 cm^{-1} [amide II (coupling of C–N stretching and N–H in-plane bending modes)] and so on. As seen from Fig. 2, a slight difference in peak position was detected for amides V and VI bands among these compounds, reflecting probably a difference in hydrogen bond strength. On heating up these samples, the bands characteristic of the α form were found to shift the positions. Fig. 3(a)–(c) show the temperature dependence of the vibrational frequencies of amide A, amide V and amide VI bands estimated for N1010CC, N1010NN and Nylon10/10, respectively. In the case of N1010CC, both the amide V and VI bands shifted to higher frequency side with increasing temperature. According to the normal modes calculation [33], the amide V and VI modes are sensitive to the slight change in the torsional angles about the amide–CH_2 bonds. The high frequency shifts of these bands suggest, therefore, the N1010CC molecule experiences larger twisting motion about the CH_2–CO and CH_2–NH bonds in higher temperature region. In particular above 60 °C, this motion seems more drastic as seen from remarkable frequency shift. In the case of N1010NN, such a high frequency shift was observed only for the amide VI band. The amide V band did not show very large frequency shift even in the high temperature region, that is to say, the twisting motion is speculated to occur mostly around the CH_2–CO bond, whereas the CH_2–NH bond experiences a small twisting motion only. In the case of Nylon 10/10, the amide V and VI bands showed a higher frequency shift in a wide temperature region of 50–140 °C and experienced further shift above 140 °C or in the Brill transition region. Fig. 4 shows the temperature dependence of infrared spectra in the regions of CH_2–CO bond stretching mode (ν[C–C(O)]), CH_2–N bond stretching mode [ν(C–N)] and methylene progression bands. The ν[C–C(O)] and ν(C–N)

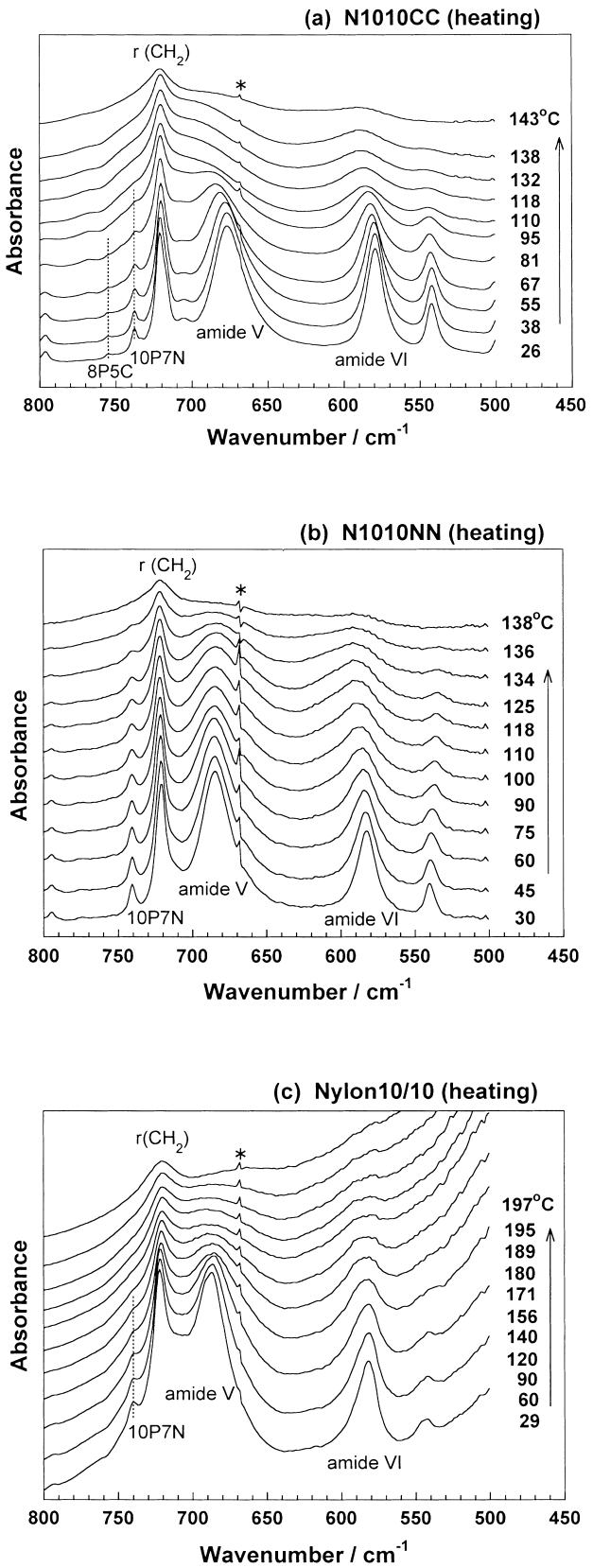

Fig. 2. Temperature dependence of infrared spectra in the frequency region of 450–800 cm^{-1}: (a) N1010CC, (b) N1010NN, and (c) Nylon 10/10. Asterisks indicate the band of CO_2 gas.

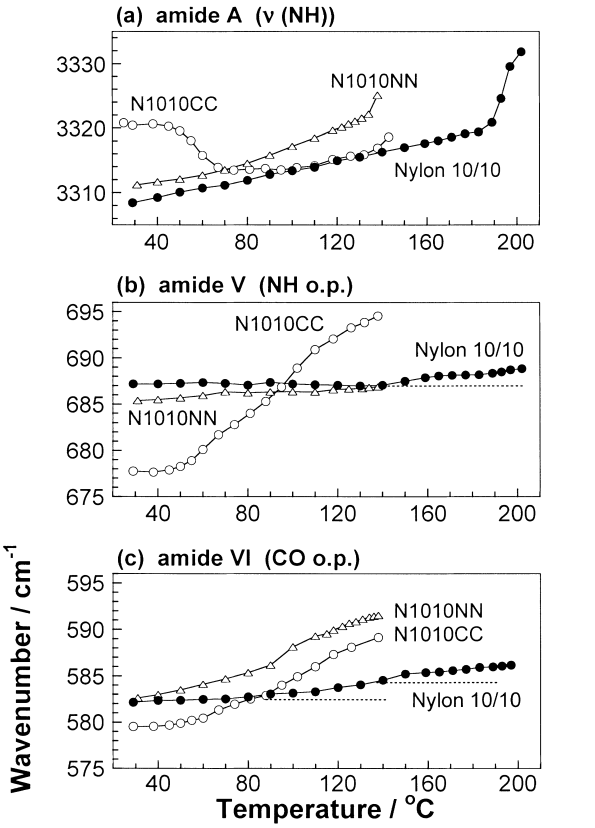

Fig. 3. Temperature dependence of the vibrational frequencies of (a) amide A, (b) amide V and (c) amide VI bands estimated for N1010CC, N1010NN and Nylon 10/10.

bands decreased in intensity remarkably with increasing temperature, in particular above the transition region. Fig. 5 shows the half-width of ν[C–C(O)] band plotted against temperature. As the temperature increased the half-width became larger for the three samples. In the Brill transition region, the half-width increased furthermore in the cases of N1010CC and Nylon 10/10. In case of N1010NN, such a remarkable increase of half-width was difficult to detect because the Brill transition was quite close to the melting point. An increment of half-width is considered to indicate an enhancement of torsional motion around the CH_2–C(O) bond, consistent with the observation made for the amide VI band. The similar observation was made also for ν(C–N) band, which decreased in intensity drastically in the Brill transition regions of N1010CC and Nylon 10/10. The N1010NN showed smaller change in a wide temperature region. The intensity reduction of ν(C–N) band is considered to reflect the enhanced torsional motion around the CH_2–NH bond, consistent with the behavior of amide V band.

As shown in Fig. 3(a), amide A band originates from the NH stretching mode and relates with the strength of the intermolecular hydrogen bonds. For N1010CC, the 3320 cm^{-1} band shifted largely to 3314 cm^{-1} at ca. 60 °C, almost the same position with those of N1010NN and Nylon 10/10. With increasing temperature this amide A band

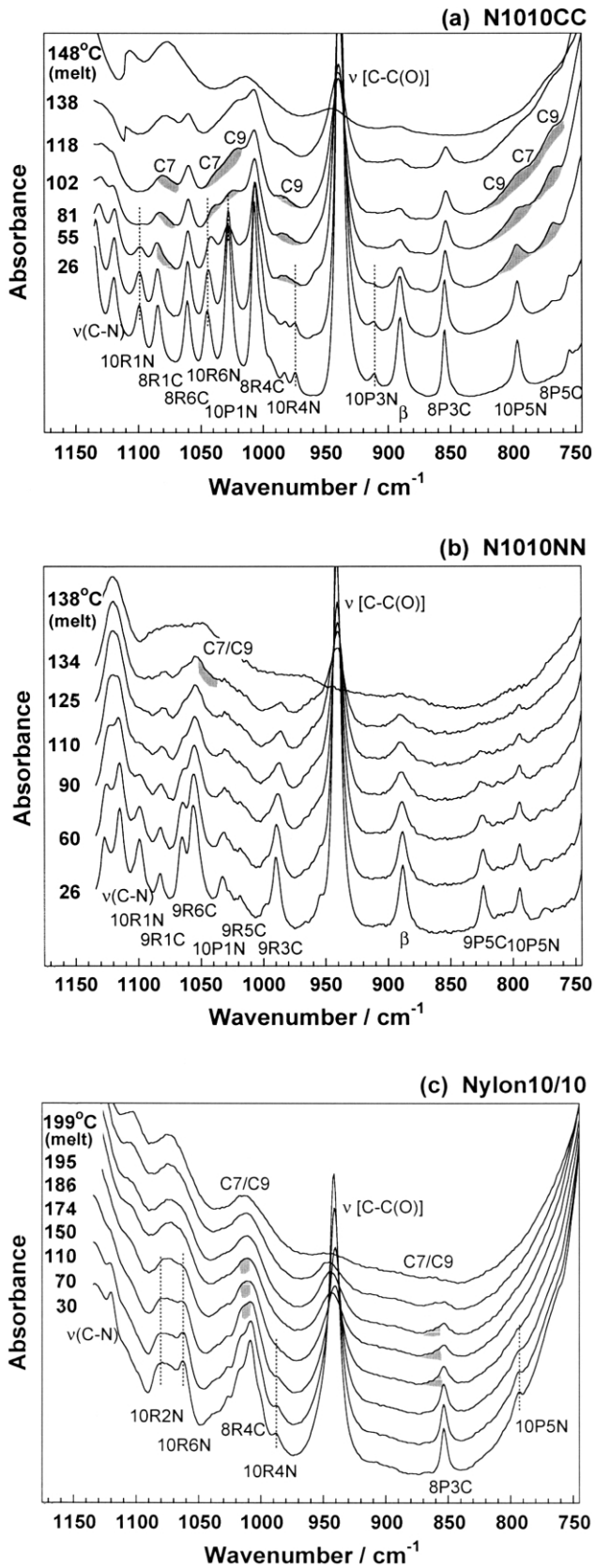

Fig. 4. Temperature dependence of infrared spectra in the frequency region of 750–1170 cm^{-1}: (a) N1010CC, (b) N1010NN, and (c) Nylon 10/10. The marks indicate the vibrational modes assigned to the methylene progression bands: for example, 10P1N indicates the rocking-twisting mode (P) of the methylene segment in the NH side (N) with $k = 1$ or the phase angle $\phi = \pi/9$, which is equivalent to the normal mode of n-$C_{10}H_{22}$ chain. C7 and C9 indicate the bands corresponding to those of n-C_7H_{16} and n-C_9H_{20}, respectively. β indicates the rocking mode of the end methyl group.

shifted gradually to the higher frequency side, reflecting the weakening of the intermolecular hydrogen bond strength. In this way, the hydrogen bonds of N1010CC are considered to become stronger once around 60 °C and then become weaker gradually above 60 °C. In the case of N1010NN and Nylon 10/10, amide A band shifted monotonically to higher frequency side with increasing temperature and no deflection of the curve was observed even in the Brill transition region. The band shifted more largely in the melting region, indicating that the intermolecular hydrogen bonds became much weaker in the melt. The new NH stretching band was observed at 3450 cm^{-1} in the melting region, which corresponded to the hydrogen-bond-free amide group. That is to say, the intermolecular hydrogen bonds were broken partly as the temperature approached the melting point.

3.2.2. Methylene progression bands

Relatively sharp band of methylene rocking mode was observed at ca. 722 cm^{-1} commonly in the spectra of Nylon 10/10 and model compounds as shown in Fig. 2(a)–(c). This band is typical of the triclinic packing structure of *n*-alkane [43–45]. Therefore, the subcell of methylene sequences of Nylon 10/10 and model compounds is considered to take the triclinic packing structure, which is consistent with the X-ray diffraction data presented in a later section. With increasing temperature, the band shifted gradually toward the position characteristic of the hexagonal packing (ca. 721 cm^{-1}) [43–47] but this approach was not completed. The similar phenomenon could be observed also in the methylene scissoring region of 1460–1490 cm^{-1}, although the spectra are not reproduced here. These spectral changes indicate that the triclinic packing structure of methylene segments approaches gradually the hexagonal packing structure in higher temperature region.

In Fig. 4(a)–(c) many bands are assigned to the progression bands of CH_2 rocking and C–C stretching modes of methylene sequences. The vibrational frequency is dependent on the phase angle ϕ between the neighboring methylene groups (or oscillators), where ϕ is determined by an effective length of the planar-zigzag methylene segment: $\phi = k\pi/(m+1)$ [m is the number of methylene units and $k = 1, 2, \ldots, m$]. It is possible to relate most of the observed progression bands to the infrared bands observed for *n*-alkanes of planar-zigzag conformation [48–52]. But, as reported in the previous paper [32], not all the methylene units of a segment can be included in this band assignment. Rather the methylene group adjacent to the amide group is needed to be distinct from the inner methylene segments. In

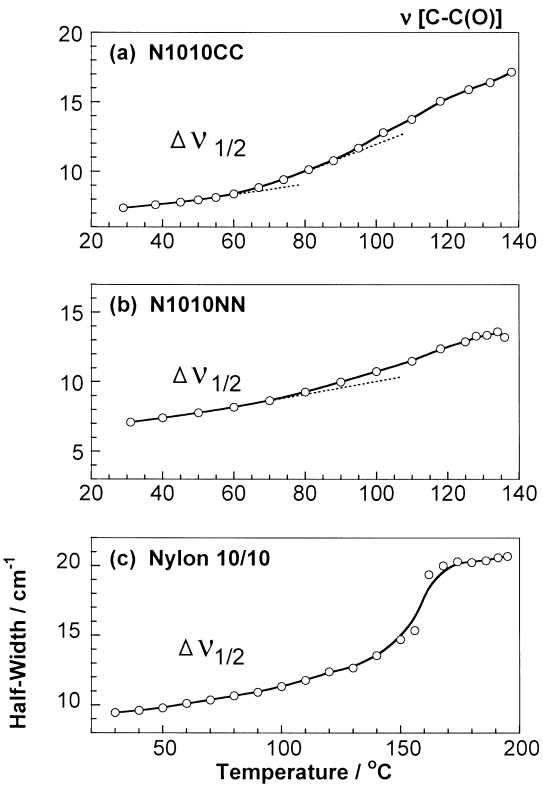

Fig. 5. Temperature dependence of half-width of infrared ν[C–C(O)] band estimated for (a) N1010CC, (b) N1010NN, and (c) Nylon 10/10.

other words, the inner methylene segments form a standing wave of vibrations almost independently of the methylene groups connected directly to the amide groups. For example, for the planar-zigzag methylene chain of Nylon 10/10, the methylene sequence NH–$(CH_2)_{10}$–NH can be separated to –$(CH_2)_8$– and two CH_2–NH units from the viewpoint of vibrational modes. The similar separation must be made also for CO$(CH_2)_8$CO; –$(CH_2)_6$– and 2 CH_2–CO units. The –$(CH_2)_8$– and –$(CH_2)_6$– segments are assumed to be equivalent to n-$C_{10}H_{22}$ [CH_3–$(CH_2)_8$–CH_3] and n-C_8H_{18} [CH_3–$(CH_2)_6$–CH_3], respectively. The progression bands assigned to the vibrational modes of equivalent n-alkanes are indicated by small symbols in Fig. 4. For example, 10P1N means that this band is equivalent to the progression band of CH_2 rocking (P) mode with a phase angle between the neighboring methylene groups $\phi = k\pi/(m+1) = 1 \times \pi/(8+1) = \pi/9$ [a total number of effective oscillators m = 8 and $k = 1$]. A chain having eight methylene groups is equivalent to n-$C_{10}H_{22}$ when two methyl groups are added as end groups, corresponding to Fig. 10 at the head of symbol. The 'N' indicates that it is a mode of the methylene sequence of the NH group side [NH–$(CH_2)_{10}$–NH].

When the samples were heated the progression bands decreased in intensity, reflecting a conformational fluctuation or conformational disordering in higher temperature region. These bands showed also the vibrational frequency shifts. In the Brill transition region, some of the progression bands continued to decrease in intensity but some bands disappeared perfectly. At the same time new bands were detected instead. Before analyzing these observations, it is needed to know the physical meanings of these spectral changes.

In the vibrational frequency-phase angle dispersion curve of a particular mode, the vibrational frequency ν is determined uniquely when a phase angle ϕ is given [52–54]. As mentioned already, the ϕ is determined by the number of oscillators (m) or the length of methylene zigzag chain segment. Therefore, when the methylene chain length becomes shorter, the ϕ is modified and then the ν is changed. For example, when a large conformational disordering occurs by an invasion of *gauche* bonds, the effective length of planar-zigzag methylene segment is shortened. Then, the progression bands corresponding to the original segment disappear and the new progression bands appear at different positions determined by the phase angles predicted for the newly-attained *trans* segmental length. However, even when such a large conformational change does not occur but only small conformational fluctuation of a chain occurs, the effective chain length may be changed more or less. In this case the change of vibrational frequency is quite small and so the band looks to shift its position continuously. The conformational fluctuation causes an orientational fluctuation of transition dipole, resulting in the decrease in intensity of the corresponding infrared band because the intensity is proportional to the square of the transition dipole of the vibrational mode in question. In this way, the thermal fluctuation of a regular chain segment causes the apparent frequency shift and the decrease in infrared band intensity, while the more remarkable conformational disordering due to the *trans–gauche* exchange causes the disappearance of the original progression bands and the appearance of new progression bands. By taking these situations into consideration, we will now investigate the observed behavior of the progression bands concretely (Fig. 4).

In the case of N1010CC, most of the progression bands decreased in intensity gradually with increasing temperature (below 60 °C), suggesting an increasing conformational fluctuation of the *trans*-zigzag methylene segmental parts. Once the sample was heated up to the Brill transition region of 70–110 °C, some of the progression bands disappeared and some other bands still continued to decrease in intensity. The formers are 10P7N (738 cm^{-1}), 10P3N (911 cm^{-1}), 10R4N (974 cm^{-1}), 10P1N (1028 cm^{-1}), 10R6N (1045 cm^{-1}), 10R1N (1100 cm^{-1}), 10W1N (1207 cm^{-1}), 10T4N (1275 cm^{-1}) and so on, where R, W and T indicate the CC stretching mode, the methylene wagging mode and the methylene twisting mode, respectively. It is noticed here that most of these bands come from the methylene segments of the NH side [CH_3–$(CH_2)_9$NH]. The progression bands assigned to the CO side [CO–$(CH_2)_8$–CO] did not disappear but decreased in intensity even above the transition point (e.g. 8P3C, 8R4C and 8R6C). Fig. 6(a) shows the temperature dependence of the infrared intensity

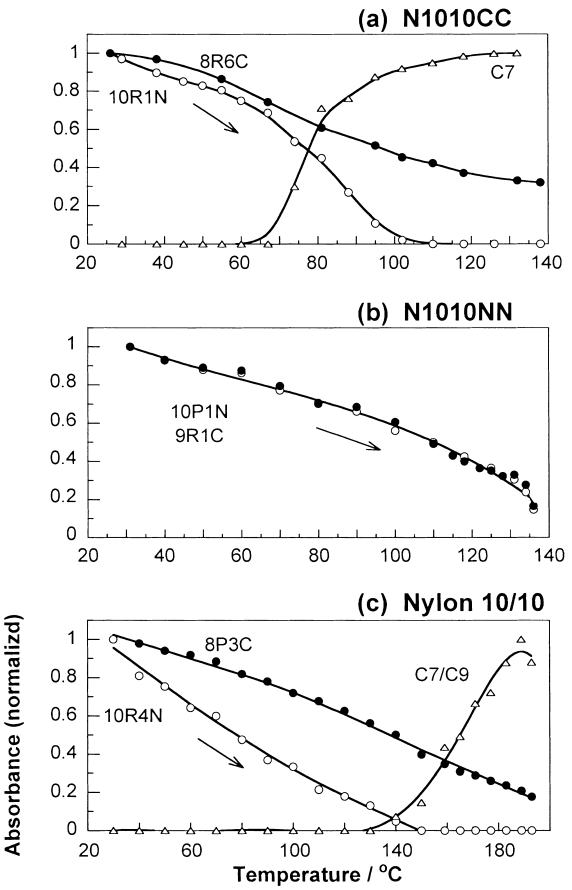

Fig. 6. Temperature dependence of infrared band intensity of several progression bands: (a) N1010CC, (b) N1010NN, and (c) Nylon 10/10 (refer to Fig. 4). The absorbance is normalized by the maximal value.

estimated for several progression bands of N1010CC. The intensity of the progression bands coming from the methylene segment of NH side (10R1N in this figure) decreased with increasing temperature and the decreasing rate was higher above 60 °C and disappeared perfectly above 100 °C. The intensity of the methylene bands of the CO side (8R6C) decreased gradually in a wide temperature region but did not disappear up to the melting point. In addition to these changes, new bands were observed to appear in the high-temperature region (Fig. 4(a)). These new bands were corresponded relatively well to the bands of *n*-C_9H_{20} and *n*-C_7H_{16} [51–54]. That is to say, the fully *trans*-zigzag methylene sequence of the NH side changed to the shorter zigzag segments of $(CH_2)_7$–$(CH_2)_5$. The generation of *gauche* bands could be also detected around 1454 cm^{-1} above 100 °C [44–47]. From these observations it may be said that the long zigzag methylene segments change the conformation to the disordered structure consisting of shorter *trans* segments combined with the *gauche* bonds.

As mentioned above, the bands assigned to the methylene segments of NH side showed more remarkable intensity change than those of CO side in the Brill transition region. This observation is consistent with the solid-state NMR data measured for Nylon 6/6 [55,56]: the methylene segments of the NH side change their thermal mobility more remarkably than those of the CO side. The methylene segments of the NH side are considered to experience a drastic conformational change to the disordered form above 100 °C.

The similar phenomenon was observed for Nylon 10/10, although it was difficult to detect the new bands because of their broadness. Fig. 6(c) shows the temperature dependence of the infrared intensity estimated for some progression bands of Nylon 10/10. The band (10R4N at 988 cm^{-1}) decreased in intensity in the wide temperature range of 40–140 °C and disappeared in the Brill transition region. The bands of 10R6N (1040 cm^{-1}), 10R2N (1062 cm^{-1}), 10W1N (1203 cm^{-1}), 10T4N (1273 cm^{-1}) and so on were found also to disappear. The 8P3C band decreased in intensity but did not disappear up to melting. New bands were observed above 140 °C at 858, 1012 and 1196 cm^{-1}, which were assigned to the progression bands of *n*-C_9H_{20}–*n*-C_7H_{16}. In this way, Nylon 10/10 is considered to transform to the conformationally-disordered form consisting of shorter zigzag segments of $(CH_2)_7$–$(CH_2)_5$ above 140 °C. Even in lower temperature region of 40–140 °C, however, the progression bands decreased in intensity with increasing temperature, indicating an occurrence of thermal fluctuation or small degree of conformational disordering of the methylene segments. A broad endothermic output in the DSC (Fig. 1) may correspond to this structural change.

In the case of N1010NN shown in Fig. 6(b), the behavior of the methylene progression bands was essentially the same for both the NH and CO sides and did not disappear even at a high temperature. But, some conformational disordering is considered to occur more or less in a wide temperature region of 70–130 °C as understood from the gradual decrease in intensity of the progression bands. The broad DSC peak detected in Fig. 1 corresponds to this change. In a quite narrow temperature region immediately below the melting point these bands showed more rapid decrease in intensity and disappeared finally in the melting region. At the same time some new bands were detected at the positions corresponding to the bands of *n*-C_7H_{16}–*n*-C_9H_{20} but they were quite broad and overlapped with the bands of the melt. Therefore, the quantitative evaluation of intensity was not made. Anyway it may be said that some drastic conformational disordering occurs just below the melting region.

3.3. Temperature dependence of X-ray diffraction pattern

Fig. 7(a) shows the temperature dependence of X-ray diffraction profile measured for N1010CC. The diffraction profile is too complicated to analyze straightforwardly for getting the concrete crystal structure. But some characteristic peaks can be picked up which are considered to reflect a packing mode of methylene segments. At room temperature the main three peaks detected at $2\theta = 20.0$, 23.8 and 25.0° seem to correspond to the $(010)_s$, $(100)_s$ and $(1\bar{1}0)_s$ peaks,

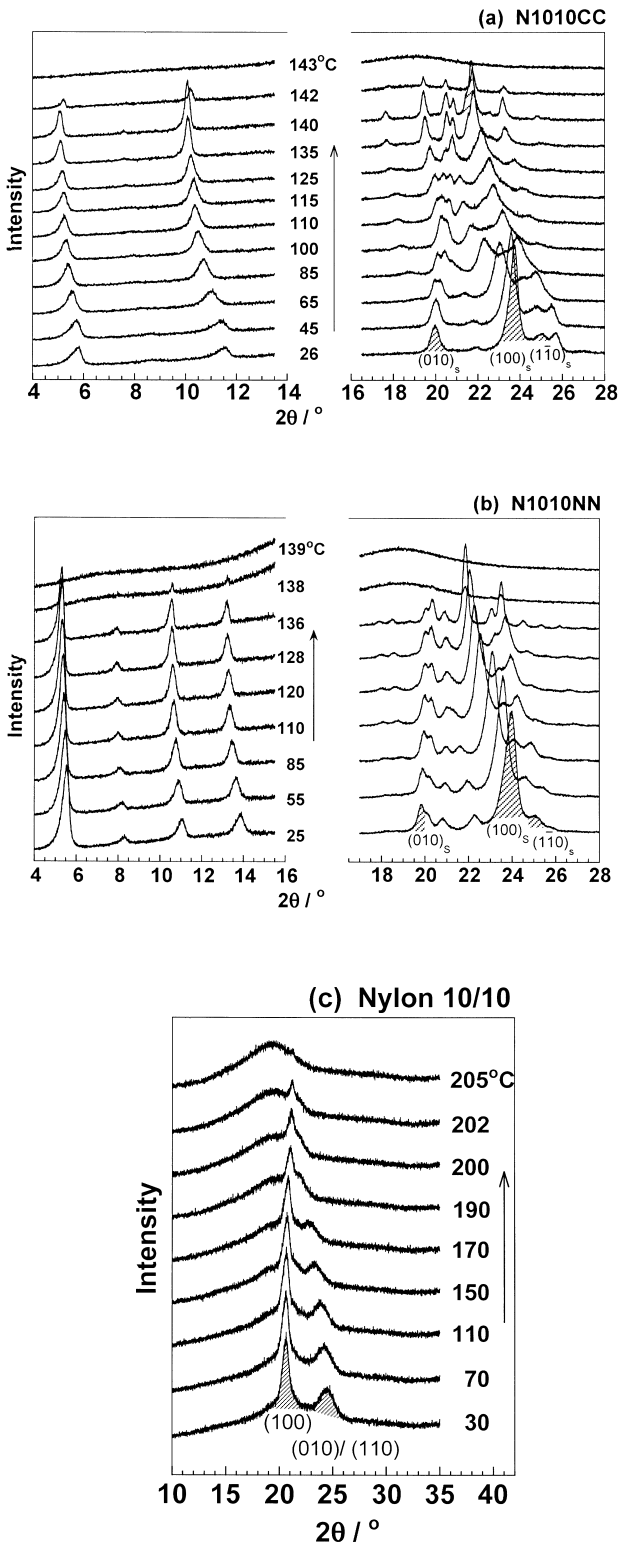

Fig. 7. Temperature dependence of X-ray diffraction profile: (a) N1010CC, (b) N1010NN, and (c) Nylon 10/10. The $(hkl)_s$ is an index for the subcell structure of the methylene segmental parts on the basis of the unit cell of *n*-alkane [57,58].

respectively, which are typically observed for triclinic subcell structure of *n*-alkanes (subscript 's' indicates the subcell). The unit cell parameters of the sub lattice are estimated as $a'_s = a_s \sin \beta'_s = 4.00$ Å, $b'_s = b_s \times \sin \alpha'_s = 4.75$ Å and $\gamma'_s = 111.3°$, which correspond relatively well to the triclinic cell parameters of *n*-alkanes: $a'_s = 4.07$ Å, $b'_s = 4.74$ Å and $\gamma'_s = 111.2°$ [57–59]. This is consistent with the information obtained by infrared spectra data (722 cm^{-1} band in Fig. 2(a)). From a series of reflections observed in the low scattering angle region, the molecular chains are considered to form a stacked layer structure. The long spacing of this layer structure is about 30.6 Å at room temperature. By taking into account the chain length of fully-extended conformation, 43.4 Å, a chain is considered to tilt by about 45° from the normal to the layer plane. As the temperature increased, the X-ray diffraction pattern showed the drastic change. The temperature dependence of the lattice spacings of the $(010)_s$, $(100)_s$ and $(1\bar{1}0)_s$ diffractions is shown in Fig. 8 in comparison with the DSC thermogram, infrared absorbance and so on. The reflections started to approach each other around 60 °C and almost merged into

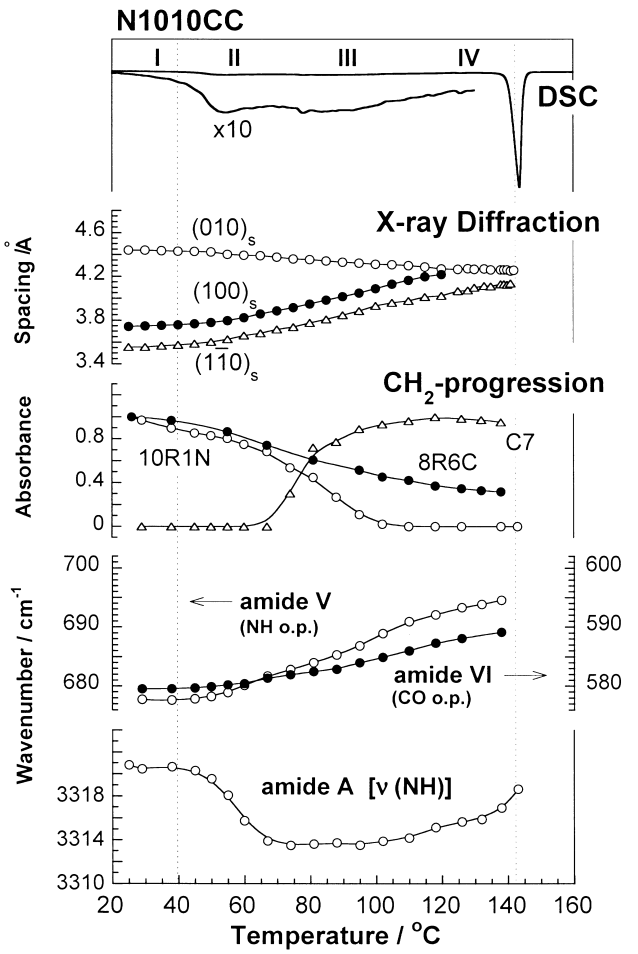

Fig. 8. Temperature dependence of the various experimental data collected for N1010CC: the DSC thermogram, the X-ray lattice spacings, the intensity of the progression bands and the wavenumbers of amide V, amide VI and NH stretching bands.

one above 110 °C. Detailed discussion about Fig. 8 is made in a later section.

Quite different behavior is observed in the N1010NN case shown in Fig. 7(b). The subcell has a dimension of $a'_s = 3.96$ Å, $b'_s = 4.80$ Å and $\gamma'_s = 110.9°$ at room temperature. The long spacing of the layer structure was estimated to be 32.0 Å from the data in low scattering angle, indicating a tilting angle of about 42°. As plotted in Fig. 9, the lattice-spacings of the subcell showed mostly the thermal expansion behavior and the reflections did not merge into one even in the high temperature region. Strictly speaking, the lattice spacings of these reflections tend to change the slope around 70 °C and come gradually closer, showing a tendency to approach the pseudo-hexagonal structure. As mentioned in Fig. 5, 70 °C corresponds to the temperature region where the ν[C–C(O)] band started to change its half-width and also to the very small endothermic peak of DSC thermogram (Fig. 1).

In the case of Nylon 10/10 [see Figs. 7(c) and 10] the reflections $(010)_s$ and $(100)_s/(1\bar{1}0)_s$ ($a'_s = 4.00$ Å, $b'_s = 4.73$ Å and $\gamma'_s = 115.0°$), which correspond to the reflections of

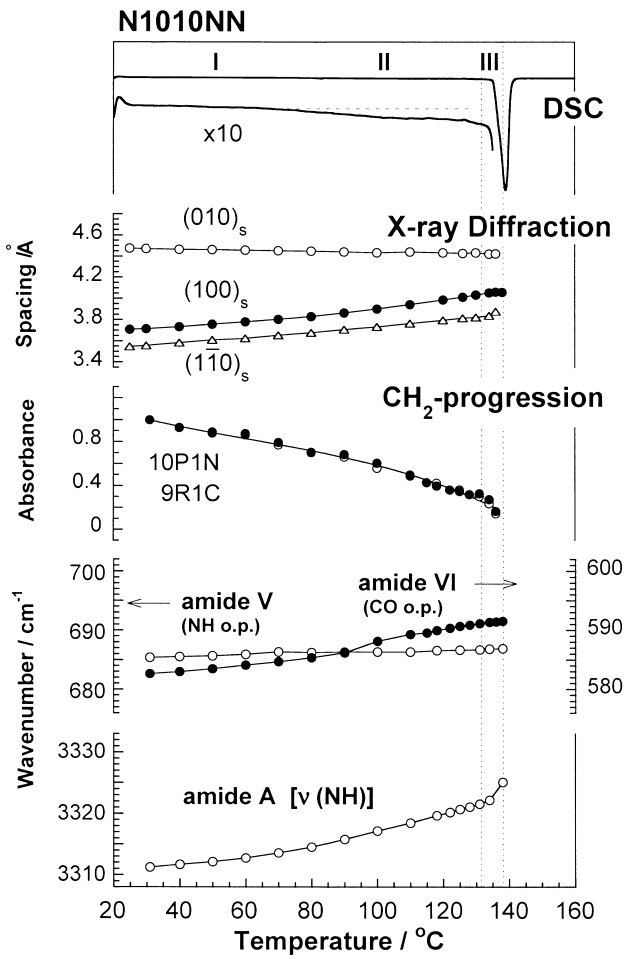

Fig. 9. Temperature dependence of the various experimental data collected for N1010NN: the DSC thermogram, the X-ray lattice spacings, the intensity of the progression bands and the wavenumbers of amide V, amide VI and NH stretching bands.

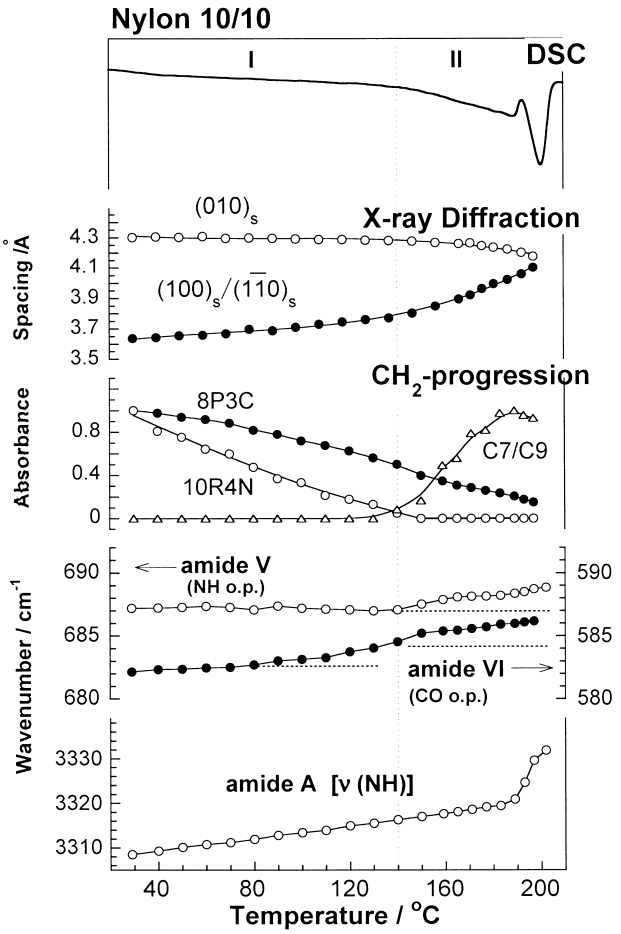

Fig. 10. Temperature dependence of the various experimental data collected for Nylon 10/10: the DSC thermogram, the X-ray lattice spacings, the intensity of the progression bands and the wavenumbers of amide V, amide VI and NH stretching bands. The $(100)_s$, $(010)_s$ and $(110)_s$ reflections correspond to the (010), (100) and (110) of the crystal lattice of Nylon 10/10, respectively [15,34].

(100) and (010)/(110) of the original lattice of Nylon m/n [15,34], showed simple thermal expansion behavior below 140 °C, above which however a remarkable change of the slope was detected and these reflections approached together to merge into one reflection characteristic of the pseudo-hexagonal lattice [57,58]. But, before completion of this transition, the crystallites were melted above 205 °C.

3.4. Crystal structural changes in the Brill transitions

In Figs. 8–10 the temperature dependences of various kinds of data are compared together: the DSC thermogram, the lattice spacings, the intensity of the progression bands and the wavenumbers of amide A, amide V and amide VI bands. The temperature dependence of ν[C–C(O)] and ν(C–N) bands is also useful for discussion [Figs. 4 and 5].

In the case of N1010CC shown in Fig. 8, the temperature region may be divided roughly into four before the melting. In the region I, almost no change was detected but only the small thermal expansion was observed for the X-ray lattice

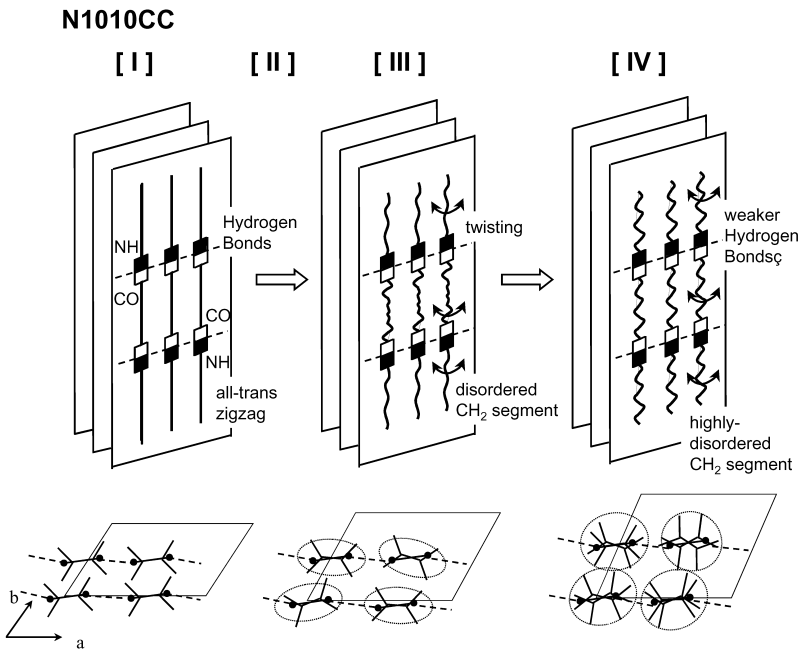

Fig. 11. An illustration of the structural change in the phase transition process of N1010CC. Refer to the temperature regions shown in Fig. 8. The small squares indicate the amide groups. The conformational change of a methylene part is given as a change of a string shape. The intermolecular hydrogen bonds are kept alive in these phase transitions.

spacings. The structure was of the α form type. In the region II, the lattice spacing of the triclinic sublattice of the methylene segments started to expand more largely. At the same time the progression bands of the methylene segments of NH and CO sides started to decrease in intensity, suggesting a start of conformational fluctuation in the methylene segments. The NH stretching band (amide A) showed a remarkable low frequency shift, indicating an increment of the hydrogen bond strength. Amide V and VI bands started to shift the peak positions, suggesting a change in torsional angles of amide–CH_2 bonds. The endothermic peak of DSC around 60 °C corresponds to these structural changes. In the region III, more remarkable change was observed for the $(100)_s$ and $(1\bar{1}0)_s$ lattice spacings and the subcell structure started to change toward the pseudo-hexagonal form. The methylene progression bands of the NH side decreased in intensity remarkably, and new bands corresponding to $(CH_2)_7$–$(CH_2)_5$ segments started to appear at the same time. The hydrogen bond strength did not change very much as seen from the constancy of NH stretching band frequency. The infrared bands of amide V, VI, ν[C–C(O)] and ν(C–N) modes showed larger changes. The conformational disordering of the whole chain occurred drastically but with keeping the hydrogen bonds. The methylene segment of the NH side experienced higher degree of conformational disordering than that of the CO side. In the region IV, the $(1-10)_s$ and $(110)_s$ spacings were almost coincident and a pseudo-hexagonal structure was attained as for the methylene segmental parts. The progression bands of the NH side disappeared almost perfectly, and the new bands of shorter zigzag segments and the *gauche* bands increased the intensity, indicating larger conformational disordering in the methylene segments. The hydrogen bonding became weaker with increasing temperature.

The above-mentioned structural changes are shown in Fig. 11. The structure of α form in region I starts to disorder in region II, but only slightly. In region III, the methylene conformation of CH_3–$(CH_2)_9$–NH segment is disordered more remarkably than that of CO–$(CH_2)_8$–CO segment. The remarkable twisting motions around CH_2–NH and CH_2–CO bonds are also started. But, during this conformational disordering process, the hydrogen bonds between the amide groups of the adjacent chains are kept unchanged. In region IV, these structural disordering are more enhanced. The degree of disordering is still higher in CH_3–$(CH_2)_9$–NH part than CO–$(CH_2)_8$–CO part. The intermolecular hydrogen bonds become weaker. The packing of methylene segments is close to the pseudo-hexagonal type.

In the case of N1010NN shown in Fig. 9, the structural change was small in the temperature region of 30–70 °C (region I) and mostly the thermal expansion occurred. But, judging from the gradual decrease in progression band intensity and the increase in half-width of ν[C–C(O)] band (Fig. 5), the thermal motion of the methylene segments is considered to be increased gradually with increasing temperature. In region II, the twisting motion around the CH_2–CO bond was activated but it was not very much for the CH_2–NH bond. This difference of motional enhancement seems to come from such a situation that the methylene segment of the NH side is sandwiched by two

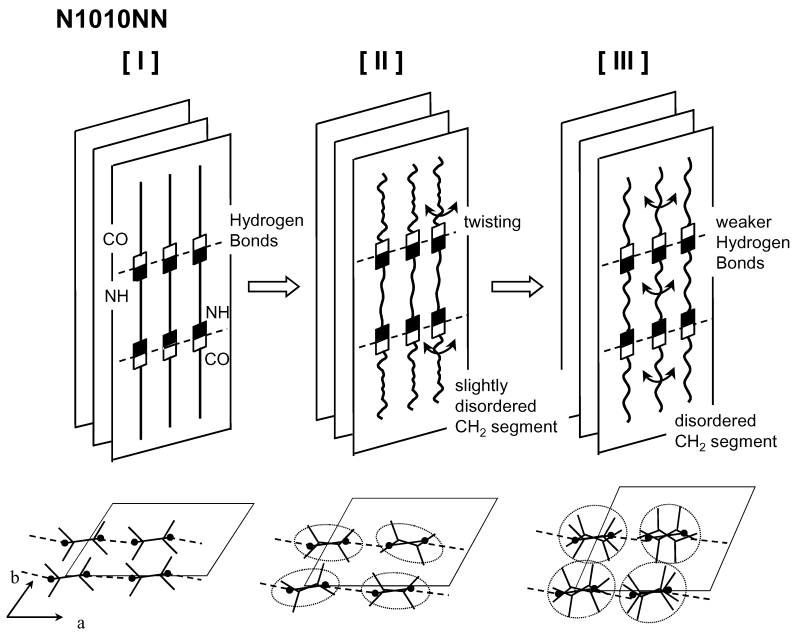

Fig. 12. An illustration of the structural change in the phase transition process of N1010NN. Refer to the temperature regions shown in Fig. 9.

hydrogen-bonded NH groups but that of the CO side is fixed to only one amide group and the other end is a methyl group. The hydrogen bonds are weakened gradually. The packing of methylene segments tends gradually to change toward the pseudo-hexagonal form. In a narrow region immediately below the melting point (region III) a conformational disordering seems to occur followed by a weakening of hydrogen bond strength, although it is not clear due to the overlap of the melt. Fig. 12 shows this structural change schematically.

The transition behavior of Nylon 10/10 is summarized in Fig. 10. In the temperature region I, the thermal expansion was observed for the subcell structure. The lattice spacing of $(100)_s/(1\bar{1}0)_s$ reflection, corresponding to the spacing between the neighboring sheets, showed a larger expansion than that of the $(010)_s$ reflection directing along the hydrogen bonds. As seen from the decrease in the progression band intensity, the methylene segments, in particular the segments of the NH side are considered to be disordered remarkably. At the same time the hydrogen bonds became weaker. The broad DSC endotherm corresponds to these changes. In the temperature region II, the lattice spacing of the $(100)_s/(1\bar{1}0)_s$ reflection expanded more remarkably and the structure approached the pseudo-hexagonal type. In the methylene segmental parts the remarkable conformational disordering was caused, as seen from the disappearance of the progression bands assigned to the long zigzag methylene chains and the appearance of new progression bands of shorter methylene segments. Judging from the temperature dependence of the progression bands, the methylene segments of the NH side are speculated to show more remarkable conformational disordering or thermal motion than those of the CO side. The twisting motion around the CH_2–CO and CH_2–NH bonds was also enhanced at the same time. Compared with the case of N1010CC, these motions are not very activated because both the segments of NH and CO sides are geometrically constrained by amide groups. The intermolecular hydrogen bonds became weaker but were not broken. An endothermic peak in a wide temperature range of 140–190 °C corresponds to these structural changes. The transformation to the perfect pseudo-hexagonal phase was not completed before the melting. Fig. 13 shows this situation schematically.

When all these structural changes are compared together, we may say as follows.

(i) In the Brill transition the methylene segments show remarkable conformational disordering. This disordering is more drastic for the methylene segments of the NH side than those of CO side.
(ii) The twisting motion about the CH_2–amide bonds becomes more enhanced in higher temperature region. In the Brill transition region this motion is enhanced furthermore (region III of N1010CC and region II of Nylon 10/10).
(iii) In parallel to the conformational disordering of molecular chains, the remarkable change occurs in the lattice spacings of the methylene subcell structure from triclinic to pseudo-hexagonal form, though not necessarily perfect.
(iv) The hydrogen bonds become weaker but are not broken even in the Brill transition region. They are broken for the first time in the melting region.

It should be noticed that the structural changes listed above ((i)–(iv)) occur in a wide temperature region even for the low-molecular-weight compounds, for example region

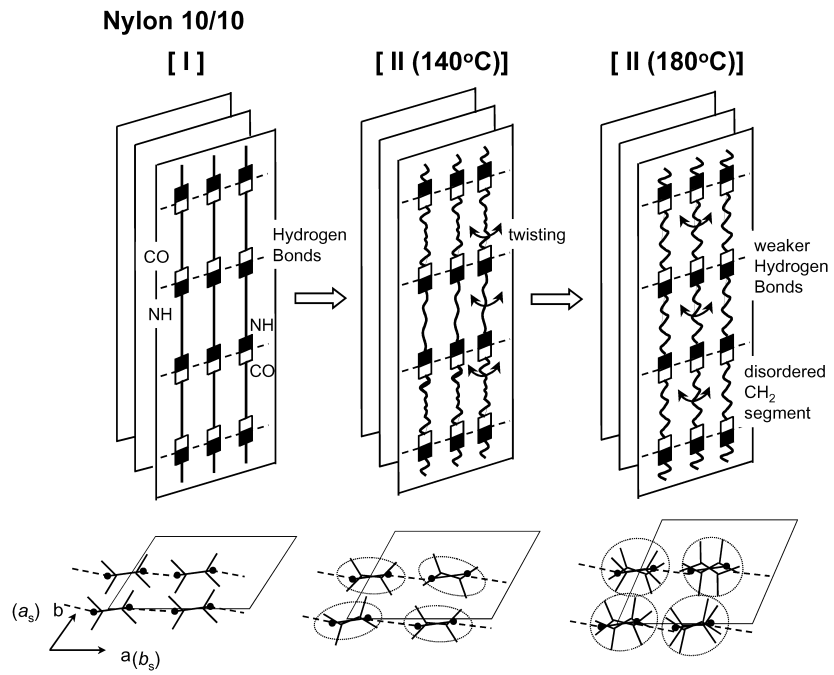

Fig. 13. An illustration of the structural change in the phase transition process of Nylon 10/10. Refer to the temperature regions shown in Fig. 10.

III in Fig. 8. This broad structural change does not come from the broad distribution of the crystallite size originated from the characteristic feature of the polymer sample, as judged from the similar observation for the low-molecular-weight model compounds. So far the Brill transition had been defined on the basis of the X-ray diffraction data as the 'perfect' transition from triclinic lattice structure to pseudo-hexagonal lattice structure, in other words, the Brill transition was considered to occur at one unique temperature. Therefore, as seen typically for the region II of Nylon 10/10 (Fig. 10), people reported that 'Nylon10/10 shows no Brill transition below the melting point' because the lattice spacings do not converge perfectly into one [15,16]. But, as seen in the two cases of N1010CC and Nylon 10/10, the methylene conformation and the torsional angles around the amide–CH_2 bonds show remarkably large change in a wide temperature region even when the pseudo-hexagonal lattice is not attained perfectly. The thermal data are also broad (Figs. 1, 8 and 10). Therefore, it may be more suitable to define 'the Brill transition' as the temperature region where the order-to-disorder structural change occurs from the α form to the structure consisting of the conformationally-disordered methylene segments and the twisted amide–CH_2 bonds with keeping the intermolecular hydrogen bonds alive.

4. Conclusions

In the present paper the structural changes in the Brill transitions of Nylon 10/10 and its model compounds were investigated systematically on the basis of the experimental data of X-ray diffraction and infrared spectra collected in the heating process from the room temperature. A series of progression bands observed at room temperature could be assigned reasonably by using a planar-zigzag conformation model for the methylene segments. In the Brill transition region, the progression bands of the NH side disappeared and new progression bands appeared. The bands of the CO side decreased in intensity but did not disappear perfectly. At the same time the *gauche* bonds were also detected to appear. From these data the conformational disordering was found to occur in the methylene segments. This conformational disordering was more drastic in the methylene segments of the NH side than those of the CO side. As a result the methylene, packing mode changed from the triclinic subcell structure to the pseudohexagonal structure, as known from the change in the X-ray reflection profile in the Brill transition region. These remarkable structural changes could be observed more easily for Nylon 10/10 and N1010CC. N1010NN was found to show this type of structural change in a narrow temperature region immediately below the melting point, although some small disordering occurred gradually even in the lower temperature region.

N1010CC and N1010NN are different only in the amide group orientation in the molecular chains. But these two compounds showed quite different transition behavior from each other. This is speculated to come from the difference in the flexibility between the methylene segments sandwiched by NH groups and those by CO groups, as reported in previous papers [25,26].

The discussion developed in the present paper seems to be useful for the investigation of the structural changes

observed in the Brill transition of the other types of nylons, as will be reported elsewhere.

Acknowledgements

The authors wish to thank Professors Yu Ding-Sheng and Jin Riguang of Beijing University of Chemical Institute for arranging the supply of Nylon 10/10 sample of the Shanghai Cellulose Works, China.

References

[1] Brill R. J Prakt Chem 1942;161:49.
[2] Itoh T. Jpn J Appl Phys 1976;15:2295.
[3] Newman BA, Sham TP, Pae KD. J Appl Phys 1976;48:4092.
[4] Starkweather HW, Jones GA. J Polym Sci, Polym Phys Ed 1981;19:467.
[5] Kim KG, Newman BA, Scheinbeim JI. J Polym Sci, Polym Phys Ed 1985;23:2477.
[6] Biangardi HJ. J Macromol Sci, Phys 1990;B29:139.
[7] Murthy NS, Curran SA, Aharoni SM, Minor H. Macromolecules 1991;24:3215.
[8] Radusch HJ, Stolp M, Androsch R. Polymer 1994;35:3568.
[9] Hill MJ, Atkins DT. Macromolecules 1995;28:2642.
[10] Jones NA, Atkins EDT, Hill MJ, Cooper SJ, Franco L. Polymer 1997;38:2689.
[11] Jones NA, Cooper SJ, Atkins EDT, Hill MJ, Franco L. J Polym Sci, Part B: Polym Phys Ed 1997;35:675.
[12] Cooper SJ, Atkins EDT, Hill MJ. Macromolecules 1998;31:8947.
[13] Franco L, Cooper SJ, Atkins EDT, Hill MJ, Jones NA. J Polym Sci, Part B: Polym Phys Ed 1998;36:1153.
[14] Murthy NS, Wang Z, Hisao BS. Macromolecules 1999;32:5594.
[15] Jones NA, Atkins EDT, Hill MJ. J Polym Sci, Part B: Polym Phys 2000;38:1209.
[16] Yang X, Tan S, Li G, Zhou E. Macromolecules 2001;34:5936.
[17] Ramesh C, Gowd EB. Macromolecules 2001;34:3308.
[18] Schneider B, Schmidt P, Wichterle O. Coll Czech Chem Commun 1962;27:1749.
[19] Jakes J, Schmidt P, Schneider B. Coll Czech Chem Commun 1965;30:996.
[20] Jakes J. J Polym Sci, Part C 1967;16:305.
[21] Jakes J, Krimm S. Spectrochim Acta 1971;27A:19.
[22] Raman R, Deopura LB, Varma DS. Indian J Text Res 1977;2:56.
[23] Vasanthan N, Murthy NS, Bray RG. Macromolecules 1998;31:8433.
[24] Cooper SJ, Coogan M, Everall N, Priestnall I. Polymer 2001;42:10119.
[25] Yoshioka Y, Tashiro K. J Phys Chem, B: in press.
[26] Tashiro K, Yoshioka Y, Hama H, Yoshioka A. Macromol Symp 2003; in press.
[27] Tereshko V, Vidal X, Goodman M, Subirana JA. Macromolecules 1995;28:837.
[28] Cooper SJ, Atkins EDT, Hill MJ. J Polym Sci, Part B: Polym Phys Ed 1998;36:2849.
[29] Cooper SJ, Atkins EDT, Hill MJ. Macromolecules 1998;31:5032.
[30] Escudero E, Subirana JA, Solans X. Acta Crystallogr 1999;C55:644.
[31] Escudero E, Subirana JA. Macromolecules 2001;34:837.
[32] Yoshioka Y, Tashiro K, Ramesh C. J Polym Sci, Part B: Polym Phys 2003;41:1294.
[33] Jakes J, Krimm S. Spectrochim Acta 1971;27A:35.
[34] Bunn CW, Garnar EV. Proc R Soc 1947;A189:39.
[35] Miyake A. J Polym Sci 1960;44:223.
[36] Arimoto H. J Polym Sci, Part A 1964;2:2283.
[37] Matsubara I, Itoh Y, Shinomiya M. Polym Lett 1966;4:47.
[38] Komatsu T, Makino D, Kobayashi M, Tadokoro H. Rep Prog Polym Phys Jpn 1970;13:1051.
[39] Skrovanek DJ, Painter PC, Colemen MM. Macromolecules 1986;19:699.
[40] Maddam WF, Royaud IAM. Spectrochim Acta 1991;47A:1327.
[41] Schmidt P, Hendra PJ. Spectrochim Acta 1994;50A:1999.
[42] Yu HH. Mater Chem Phys 1998;56:289.
[43] Snyder RG, Maroncelli M, Qi SP, Strauss HL. Science 1981;214:188.
[44] Maroncelli M, Qi SP, Strauss HL, Snyder RG. J Am Chem Soc 1982;104:6237.
[45] Maroncelli M, Strauss HL, Snyder RG. J Chem Phys 1985;82:2811.
[46] Hagemann H, Strauss HL, Snyder RG. Macromolecules 1987;20:2810.
[47] Kim Y, Strauss HL, Snyder RG. J Phys Chem 1989;93:7520.
[48] Snyder RG. J Mol Spectrosc 1960;4:411.
[49] Nielsen JR, Holland RF. J Mol Spectrosc 1960;4:448.
[50] Nielsen JR, Holland RF. J Mol Spectrosc 1961;6:394.
[51] Snyder RG, Schachtschneider JH. Spctrochim Acta 1963;19:85.
[52] Schachtschneider JH, Snyder RG. Spctrochim Acta 1963;19:117.
[53] Tasumi M, Shimanouchi T. J Mol Spectrosc 1962;9:261.
[54] Kobayashi M. J Chem Phys 1979;70:4797.
[55] Hirschinger J, Miura H, Gardner KH, English AD. Macromolecules 1990;23:2153.
[56] Wendoloski JJ, Gardner KH, Hirschinger J, Miura H, English AD. Science 1990;247:431.
[57] King HE, Sirota EB, Singer Jr. DM. J Phys, Part D: Appl Phys 1993;26:B133.
[58] Sirota EB, King HE, Singer Jr. DM, Shao HH. J Chem Phys 1995;98:5809.
[59] The sublattice of the methylene segmenetal parts is defined on the basis of the lattice parameters of *n*-alkane [57,58]. Therefore, the a_s' and b_s' axes of the subcell correspond to the b' and a' axes of the unit cell of Nylon m/n [15,34], respectively. That is to say, $(100)_s = (010)_{nylon}$ and $(010)_s = (100)_{nylon}$.